ChemPubSoc Europe

DOI: 10.1002/cphc.201800293

CHEMPHYSCHEM Communications

Like-likes-Like: Cooperative Hydrogen Bonding Overcomes Coulomb Repulsion in Cationic Clusters with Net Charges up to $Q = +6e$

Thomas Niemann,[a] Peter Stange,[a] Anne Strate,[a] and Ralf Ludwig*[a, b]

Quantum chemical calculations have been employed to study kinetically stable cationic clusters, wherein the monovalent cations are trapped by hydrogen bonding despite strongly repulsive electrostatic forces. We calculated linear and cyclic clusters of the hydroxy-functionalized cation N-(3-hydroxypropyl) pyridinium, commonly used as cation in ionic liquids. The largest kinetically stable cluster was a cyclic hexamer that very much resembles the structural motifs of molecular clusters, as known for water and alcohols. Surprisingly, strong cooperative hydrogen bonds overcome electrostatic repulsion and result in cationic clusters with a high net charge up to $Q = +6e$. The structural, spectroscopic, and electronic signatures of the cationic and related molecular clusters of 3-phenyl-1-propanol could be correlated to NBO parameters, supporting the existence of "anti-electrostatic" hydrogen bonds (AEHB), as recently suggested by Weinhold. We also showed that dispersion forces enhance the cationic cluster formation and compensate the electrostatic repulsion of one additional positive charge.

In contrast to ion pairing between ions of opposite charge, the clustering of like-charged ions seems to be an elusive concept.[1,2] It contradicts the tenet of classical electrostatics that like charges repel each other. Meanwhile, theoretical and experimental evidence is available showing the importance of this counterintuitive phenomenon in the gaseous and condensed phase.[3–11] Cationic and anionic dimers are kinetically stabilized by hydrogen bonding, opposing a "Coulomb explosion" to separate the ions. In theoretical studies of like-charge attraction, Klein and Weinhold claimed that doubly-charged complexes $[A\text{-}HB]^{2\pm}$ are manifestations of "anti-electrostatic" hydrogen bonds (AEHB), wherein the short-range donor-acceptor covalency forces overcome the powerful long-range electrostatic opposition to be expected between ions of like charge.[3–5] Weinhold analyzed the potential energy curves for the ion-ion interactions which showed shallow local minima indicating hydrogen bonding between the like-charged ions and kinetic stabilization. However, like-charge attraction in "real systems" could be only observed for large-scale structures, assemblies or stabilizing frameworks.[6–9] In solution, solvent molecules like water are required to attenuate the Coulomb repulsion.[10,11] Recently, the formation of clusters of like-charged ions in pure ionic liquids has been observed. Cationic clusters are kinetically stabilized by cooperative hydrogen bonds between the OH groups of the hydroxy-functionalized ammonium and imidazolium cations.[12–18] However, to large extent the cationic cluster formation is supported by weakly coordinating anions, which compensate for the positively charged centers of the cations and allow for counterion-meditated attraction between the likes.[17,18]

It is the purpose of the present work to study kinetically stable cationic clusters, wherein, in the absence of any mediating "solvent effects" by molecules or counterions, the repulsive Coulomb forces can be compensated merely by cooperative hydrogen bonding between the cations. We particularly want to show that like-charge attraction also exists for cationic clusters that are much larger than the reported dimers with net charge $Q = \pm 2e$.[3,4] Braga and coworkers already questioned anion-anion interaction from molecular electrostatic potential considerations and concluded that it is instead a "tugboat interaction", controlling anion aggregation and minimizing anion-anion repulsions.[19] They claimed that the anionic dimer would fall apart if the countercations are removed. However, Head-Gordon and Frenking showed that the local minimum structures for anionic dimers can be also analyzed by electronic decomposition analysis (EDA) methods.[20,21] Nevertheless, larger cationic clusters are not expected within electrostatic conception due to strongly increasing repulsive interaction with each additional positive charge.

Here, we show that larger clusters of monovalent cations up to net charges $Q = +6e$ can be kinetically trapped by cooperative hydrogen bonding. No mediating molecules, counterions or screening effects are needed to overcome the repulsive Coulomb forces. The structural, spectroscopic and electronic signatures of the cationic and related molecular clusters could be related to NBO parameters, supporting the existence of "anti-electrostatic" hydrogen bonds (AEHB) as recently suggested by Weinhold.[3–5] We also show that dispersion forces enhance the cationic cluster formation and compensate the long-range electrostatic repulsion. Overall,

[a] T. Niemann, P. Stange, Dr. A. Strate, Prof. Dr. R. Ludwig
Universität Rostock, Institut für Chemie, Abteilung für Physikalische und Theoretische Chemie,
Dr.-Lorenz-Weg 2, 18059, Rostock (Germany)
E-mail: ralf.ludwig@uni-rostock.de
[b] Prof. Dr. R. Ludwig
Leibniz-Institut für Katalyse an der Universität Rostock e.V., Albert-Einstein-Str. 29a, 18059 Rostock (Germany)

Supporting Information for this article is available on the WWW under https://doi.org/10.1002/cphc.201800293

dispersion interactions shift the kinetic stability from a cyclic pentamer to a cyclic hexamer.

For that purpose we have chosen the hydroxy-functionalized cation N-(3-hydroxypropyl) pyridinium [HPPy$^+$] and its molecular mimic 3-phenyl-1-propanol [3-Phe-1-Pr] as model systems. We calculated linear clusters up to tetramers ($n=4$) and cyclic clusters up to hexamers ($n=6$). The hydroxy groups on the cations form hydrogen bonds and promote the aggregation into highly charged cationic clusters. We employed B3LYP/6-31+G* and B3LYP-D3/6-31+G* calculations performed with the Gaussian 09 program and analyzed with the NBO 6.0 program.[22–27] For calculating all cationic and molecular clusters at the same level of theory, we have used the well-balanced, but small 6-31+G* basis set. It includes polarization as well as diffuse functions, and has been shown to be suitable for calculating hydrogen-bonded clusters of like-charged ions.[14–18] The 6-31+G* basis set is also chosen for better comparison with earlier studies of molecular and ionic clusters.[28–31] We also show that the salient properties of these clusters can be robustly calculated with both smaller und larger basis sets. This is demonstrated for the features of the largest cationic cluster found here (see calculated cyclic hexamers revealed from B3LYP-D3 calculations at 3-21G, 6-31+G* and 6-311++G** basis sets (see SI). All the pure cationic clusters [HPPy$^+$]$_n$ and molecular clusters [3-Phe-1-Pr]$_n$ were fully optimized. The calculated vibrational frequencies were all positive, showing that we calculated at least local minimum structures. Additionally, we calculated OH vibrational frequencies for the OH bonds, ν_{OH}, and the hydroxy proton chemical shifts, δ ^{1}H, for each configuration. These spectroscopic observables are related to NBO-calculated second order stabilization energy $\Delta E(2)_{n\rightarrow\sigma^*}$ and charge transfer, q_{CT}.

Kinetically Stabilized Dimers [HPPy$^+$]$_2$: For the dimer structure [HPPy$^+$]$_2$ we calculated the fully relaxed-scan potential curve at the HF/6-31+G* (I), B3LYP/6-31+G* (II), B3LYP-D3/6-31+G* (III) and MP2/6-31+G* (IV) levels of theory. The local minimum structures were found at typical H-bond distances of $R_{O\cdots H}=2.0706$ Å, $R_{O\cdots H}=1.9546$ Å, $R_{O\cdots H}=1.9124$ Å and $R_{O\cdots H}=1.9175$ Å, for the dimers I–IV (see Table 1, SI). As shown in Figure 1, a robust kinetic stability with a clear dissociation barrier of 12–13 kJ mol^{-1} is achieved for the B3LYP-D3 and the MP2 treatments. It is interesting to note that the MP2 calculations give the lowest energies and that the B3LYP calculations represent nearly the same potential energy curve if the D3 dispersion correction is taken into account.[25–27] Thus hydrogen bonds between like-charged ions are well described by dispersion-corrected DFT methods. Therefore, a cheaper

Table 1. Calculated intermolecular distances R(O···HO) and R(O···O) as well as bond angles $<$(O···HO) of the optimized dimer structures [HPPy$^+$]$_2$ using different theoretical methods but applying the same 6-31+G* basis set.

Method	R(O···HO)	R(O···O)	$<$(O···HO)
HF	2.0706	3.0096	168.68
B3LYP	1.9546	2.9084	164.60
B3LYP-D3	1.9124	2.8716	166.32
MP2	1.9175	2.8807	166.58

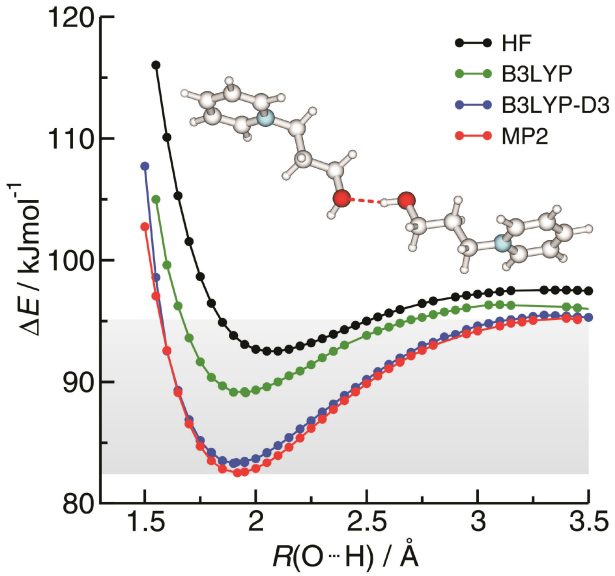

Figure 1. Potential energy curves for [HPPy$^+$]$_2$ H-bonding (all at 6-31+G* basis level) as calculated with the HF (black), hybrid density functional B3LYP (green), hybrid density functional B3LYP-D3 including dispersion correction (blue), and ab initio MP2 (red) methods. The structures were relaxed for each bond length R(O···H). The bond lengths R(O···H) at lowest energy are given in Table 1.

than MP2 level of theory can be used to describe the essential structural and energetic properties of cationic clusters without significant loss of accuracy.

Cyclic Clusters up to Net Charge $Q=+6e$: We then optimized linear and cyclic cationic clusters of [HPPy$^+$]$_n$ and [3-Phe-1-Pr]$_n$ from trimers up to hexamers ($n=3$–6) (see SI). For both the exotic ionic species as well as the familiar neutral analogues, the starting geometries of linear trimers and tetramers were optimized towards cyclic clusters, wherein cooperative H-bonding is maximized. By taking Grimme's D3 dispersion correction into account, we obtained intrinsic (meta) stable cyclic hexamers [HPPy$^+$]$_{6c}$ which exhibit a net charge of $Q=+6e$.[25–27] The meta-stable cationic clusters resemble the cyclic hexamer of [3-Phe-1-Pr] and those known for other alcohols and water.[14–18] Without including dispersion forces these highly charged hexamers show "Coulomb explosion" and dissociate during the optimization procedure. Ignoring dispersion forces leads to cyclic pentamers as largest kinetically stable ionic clusters (see SI).

The detection and control of clusters of like-charged ions may be regarded as support for the "anti-electrostatic" hydrogen bonds (AEHB) as reported recently by Weinhold and Klein.[3,4] Although Frenking and Head-Gordon could show that the local minimum structures for anionic dimers can be analyzed also by electronic decomposition analysis (EDA) methods, AEHBs are supported by spectroscopic observables, such as vibrational frequencies, ν_{OH}, and NMR chemical shifts, δ^1H.[20,21] Geometrical and spectroscopic properties of cationic and molecular clusters show similar behavior.

Bond Lengths and Spectroscopic Observables of the Cationic and Molecular Clusters: In the cationic clusters, the charge transfer from the oxygen lone pair orbital into the OH

antibonding orbital results in hydrogen bonding such as in molecular clusters but less pronounced. However, even in the six-fold H-bonded cationic cluster with $Q=+6e$, cooperative hydrogen bonding attenuates the repulsive Coulomb interaction, resulting in longer intra- and shorter intermolecular bond lengths. Despite strong electrostatic opposition, the cationic clusters show typical H-bond distances and spectroscopic signatures as known for molecular liquids. The intramolecular bond lengths, R(OH), and the intermolecular bond distances, R(H···O) and R(O···O), are shown in Figure 2 for the pure cationic

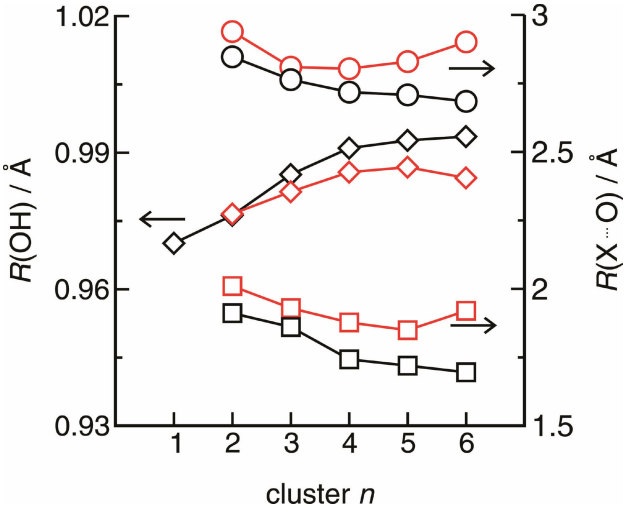

Figure 2. The intramolecular bond lengths, R(OH), (left axis, diamonds) and the intermolecular bond distances, R(H···O) (right axis, squares) and R(O···O), (right axes, circles) are shown for the molecular (black open symbols) and pure cationic clusters (red open symbols), respectively. Enhanced hydrogen bonding with increasing cluster size is observed for all systems, indicated by lengthening of the OH bonds and shortening of the intermolecular bond distances.

and the molecular clusters. Enhanced hydrogen bonding with increasing cluster size is observed. From the dimers to the cyclic tetramers, the intramolecular OH bonds are lengthened and the intermolecular distances R(H···O) and R(O···O) are shortened as expected for enhanced hydrogen bonding.[28–32] Although both effects are less pronounced in the cationic clusters, cooperativity results in typical H-bond behavior despite the strong repulsive forces.

It is interesting to note that the cationic clusters show weaker cooperativity from the cyclic tetramer on. In the higher charged cationic clusters the electrostatic repulsion becomes stronger with each additional positive charge which cannot be fully compensated by cooperative hydrogen bonding. However, also the molecular clusters show weaker cooperativity with increasing cluster size. Therein, dispersion forces strengthen the attractive interaction between the phenyl groups and indirectly weaken the hydrogen bonds of the cyclic pentamers and hexamers compared to those of the cyclic tetramer. To illustrate these effects we show the cationic hexamer in Scheme 1. The ring structure $[HPPy^+]_6$ resembles that of the water hexamer which has served for analyzing the hydrogen bond in ice. The B3LYP-D3/6-31+G* optimal geometry has an almost S_6 symmetry with four oxygen atoms lying in plane. The two remaining oxygen atoms lie on either side of this plane giving rise to a "chair" configuration.[32]

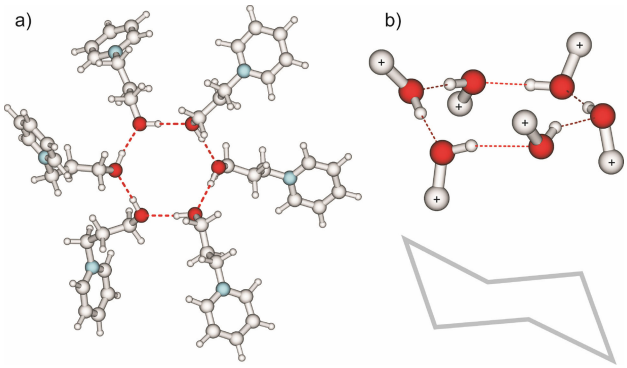

Scheme 1. Kinetically stable cationic hexamer $[HPPy^+]_6$: a) the cyclic cluster in the supervision and b) the enlarged hydrogen bonding motif of the cluster showing a "chair" configuration.

The vibrational frequencies, ν_{OH}, and the proton chemical shifts, δ^1H, for the hydroxy groups in the cationic and molecular clusters reflect this behavior in a similar way. The OH frequencies in the cyclic structures of [3-Phe-1-Pr] are substantially redshifted up to 460 cm^{-1} as shown in Figure 3a. Although weaker, the redshift due to hydrogen bonding is also observed for the cationic clusters. The OH redshift of the hexamer with $Q=+6e$ is $\Delta\nu_{OH}=280\ cm^{-1}$ and thus stronger than for the neutral [3-Phe-1-Pr] trimer. Again, cooperativity with increasing clusters size is also present for the cationic clusters. Similar behavior is observed for the proton chemical shifts which are strongly shifted downfield (see Figures 3b) compared to the corresponding monomer values. In the [3-Phe-1-Pr] clusters the hydroxy protons are strongly de-shielded, resulting in downfield chemical shifts between 5–6 ppm which is only slightly stronger than the values obtained for water and alcohols in their liquid phases.[28–30] The downfield shift of the hydroxy protons within the cationic clusters range up to 4 ppm for the cyclic pentamer/hexamer. Overall, such significant vibrational redshifts and downfield chemical shifts should be clearly observable in gas phase experiments.[33,34]

NBO Parameters and Spectroscopic Observables of the Cationic and Molecular Clusters: The B3LYP-D3/6-31+G* calculations suggest that the cation-cation interaction via the OH···OH hydrogen bond is possible due to cooperative effects.[18] Electron density from the oxygen lone pair orbital of a first cation is donated into the OH antibonding orbital of a second cation. The resulting larger negative charge at the OH oxygen at the second cation can now be transferred into the OH antibonding orbital of another cation, further enhancing hydrogen bonding. This process leads to even stronger cooperativity in the in the cyclic structures such as tetramers, pentamers and hexamers. This way, the short-range donor-acceptor covalency forces can overcome the strong long-range electrostatic repulsive forces as expected for ions of like charge. These features can be rationalized in the framework of the natural bond orbital (NBO) analysis.[23,24] NBO analysis shows

typical strong $n_o \rightarrow \sigma^*_{OH}$ donor-acceptor interaction, corresponding to second order stabilization energies $\Delta E(2)_{n\rightarrow\sigma^*}$ and estimated total charge transfers of q_{TC} for the enhanced OHLudwigOH hydrogen bonds, respectively. These typical NBO descriptors are plotted versus $\Delta\nu_{OH}$ redshifts (see Figure 4) and δ^1H downfield chemical shifts (see Figure 5). The spectroscopic features of the cationic clusters, wherein the strong repulsive Coulomb interaction is attenuated by hydrogen bonding, can be almost linearly related to the NBO descriptors. Obviously, both properties characterize hydrogen bonding and cooperativity in a similar way. IR redshifts and downfield proton chemical shifts go along with increasing stabilization energies, $\Delta E(2)_{n\rightarrow\sigma^*}$, and enhanced charge transfer, q_{CT}. That the strongest intermolecular stabilization energies are found for the cyclic structures is well correlated to the cooperative binding energies, frequencies and chemical shifts. These "closed-CT" networks have highest stability, resulting in strongest interaction, largest vibrational redshifts and strongest NMR downfield shifts.

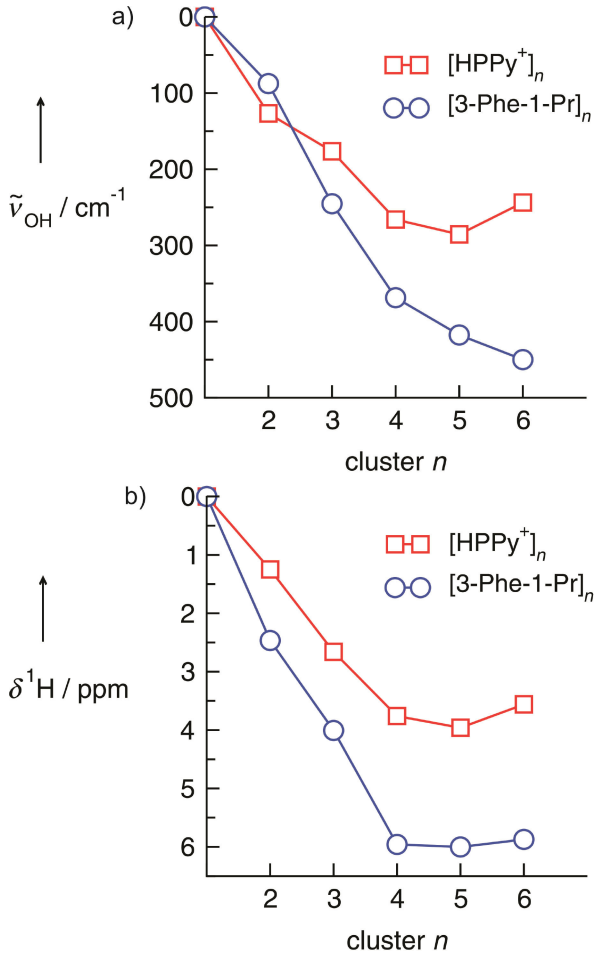

Figure 3. a) Calculated O–H vibrational redshifts, $\Delta\nu_{OH}$, for the molecular (circles) and the cationic clusters (squares) relative to the monomer values of both species. Although less pronounced, the cationic clusters show similar redshifts as the molecular clusters with increasing cluster size. Cooperative hydrogen bonding is in particular strong in the cyclic cationic tetramer. b) Calculated δ ^{1}H downfield shifts for the molecular (circles) and cationic clusters (squares) relative to the monomer values of both species. Although less pronounced, the cationic clusters show similar downfield shifts as the molecular clusters with increasing cluster size. Cooperative hydrogen bonding is in particular strong in the cyclic cationic pentamer.

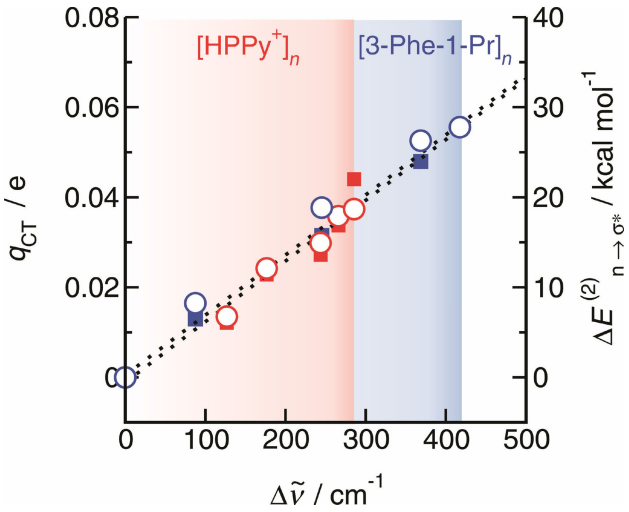

Figure 4. NBO-calculated second-order stabilization energies $\Delta E(2)_{n\rightarrow\sigma^*}$ (open circles) and estimated total charge transfers q_{CT} (closed squares) for cationic (red) and molecular (blue) clusters $n = 2$–6 plotted versus calculated redshifts of the average OH frequency, $\Delta\nu_{OH}$, of the monomeric cation and molecule. The linear dependence indicates the strong relation between NBO stabilization energies and charge transfers with spectroscopic properties such as IR frequencies. The largest redshifts for the cationic and molecular clusters are indicated by the red and blue areas.

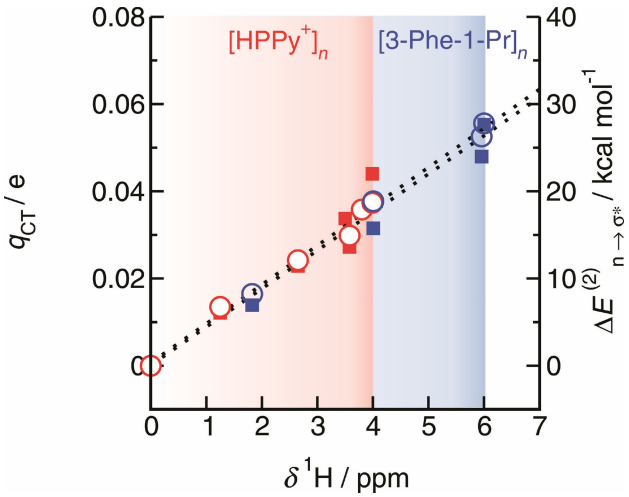

Figure 5. NBO-calculated second-order stabilization energies $\Delta E(2)_{n\rightarrow\sigma^*}$ (open circles) and estimated total charge transfers q_{CT} (closed squares) for cationic (red) and molecular (blue) clusters $n = 2$–6 plotted versus calculated average NMR proton chemical shifts, δ ^{1}H, of the monomeric cation and molecule. The linear dependence indicates the strong relation between NBO stabilization energies and charge transfers with spectroscopic properties, such as NMR chemical shifts. The largest redshifts for the cationic and molecular clusters are indicated by the red and blue areas.

In this work, we show that clusters of monovalent cations with net charges up to $Q = +6e$ are kinetically stable. Quantum chemical calculations suggest that hydrogen bonds overcome the repulsive Coulomb forces. Cooperative hydrogen bonding is in particular strong in cyclic clusters, which look similar to well-known structural motifs for water or alcohols. Coopera-

tivity is reflected in redshifted vibrational frequencies and downfield NMR chemical shifts. The cooperative effect with increasing cluster size in the cationic clusters is less pronounced, but similar to that observed in molecular clusters. Both spectroscopic probes for hydrogen bonding are linearly related to NBO-calculated interaction energies and charge transfer. This strong correlation suggests the existence of "anti-electrostatic" hydrogen bonds (AEHB) as recently introduced by Weinhold and Klein and confirmed experimentally. The present study shows that these AEHBs do not allow only the formation of ionic dimers but larger cyclic clusters with high net charges, wherein attractive short-range hydrogen bonds successfully compete with long-range repulsive Coulomb forces. Introducing dispersion forces additionally strengthens the attractive interaction and allows for the formation of cyclic hexamers with exceptionally high charge.

Acknowledgements

This work has been supported by the DFG Research Grant LU-506/14-1.

Conflict of Interest

The authors declare no conflict of interest.

Keywords: hydrogen bonding · ionic bonding · natural bond orbital analysis · spectroscopy · theoretical chemistry

[1] J. Smid, *Angew. Chem.* **1972**, *84*, 127–144; *Angew. Chem. Int. Ed.* **1972**, *11*, 112–127.
[2] Y. Marcus, G. Hefter, *Chem. Rev.* **2006**, *106*, 4585–4621.
[3] F. Weinhold, R. A. Klein, *Angew. Chem. Int. Ed.* **2014**, *53*, 11214–11217; *Angew. Chem.* **2014**, *126*, 11396–11399.
[4] F. Weinhold, *Angew. Chem. Int. Ed.* **2017**, *56*, 14577–14581; *Angew. Chem.* **2017**, *129*, 14769–14773.
[5] F. Weinhold, *Inorg. Chem.* **2018**, *57*, 2035–2044.
[6] E. M. Fatila, E. B. Twum, A. Sengupta, M. Pink, J. A. Karty, K. Raghavachari, A. H. Flood, *Angew. Chem. Int. Ed.* **2016**, *55*, 14057–14062; *Angew. Chem.* **2016**, *128*, 14263–14268.
[7] W. Zhao, B. Qiao, C.-H. Chen, A. H. Flood, *Angew. Chem. Int. Ed.* **2017**, *56*, 13083–13087; *Angew. Chem.* **2017**, *129*, 13263–13267.
[8] E. M. Fatila, E. B. Twum, J. A. Karty, A. H. Flood, *Chem. Eur. J.* **2017**, *23*, 10652–10662.
[9] W. Gamrad, A. Dreier, R. Goddrad, K.-R. Pörschke, *Angew. Chem. Int. Ed.* **2015**, *54*, 4482–4487.
[10] O. Shih, A. H. England, G. C. Dallinger, J. W. Smith, K. C. Duffey, R. C. Cohen, D. Prendergast, R. J. Saykally, *J. Chem. Phys.* **2013**, *139*, 035104.
[11] T. Inagaki, S. Aono, H. Nakano, T. Yamamoto, *J. Phys. Chem. B* **2014**, *118*, 5499–5508.
[12] S. A. Katsyuba, M. V. Vener, E. E. Zvereva, Z. Fei, R. Scopelliti, G. Laurenczy, N. Yan, E. Paunescu, P. J. Dyson, *J. Phys. Chem. B* **2013**, *117*, 9094–9105.
[13] M. Fakhraee, B. Zandkarimi, H. Salari, M. R. Gholami, *J. Phys. Chem. B* **2014**, *118*, 14410–14428.
[14] A. Knorr, K. Fumino, A.-M. Bonsa, R. Ludwig, *Phys. Chem. Chem. Phys.* **2015**, *17*, 30978–30982.
[15] A. Knorr, R. Ludwig, *Sci. Rep.* **2015**, *5*, 17505.
[16] A. Knorr, P. Stange, K. Fumino, F. Weinhold, R. Ludwig, *ChemPhysChem* **2016**, *17*, 458–462.
[17] A. Strate, T. Niemann, P. Stange, D. Michalik, R. Ludwig, *Angew. Chem. Int. Ed.* **2017**, *56*, 496–500; *Angew. Chem.* **2017**, *129*, 510–514.
[18] A. Strate, T. Niemann, R. Ludwig, *Phys. Chem. Chem. Phys.* **2017**, *19*, 18854–18862;
[19] D. Braga, F. Grepioni, J. J. Novoa, *Chem. Commun.* **1998**, 1959–1960.
[20] G. Frenking, G. F. Caramori, *Angew. Chem.* **2015**, *126*, 2632–2635; *Angew. Chem. Int. Ed.* **2015**, *54*, 2596–2599.
[21] P. R. Horn, Y. Mao, M. Head-Gordon , *Phys. Chem. Chem. Phys.* **2016**, *18*, 23067–23079.
[22] Gaussian 09, Revision A.02, M. J. Frisch, G. W. Trucks, H. B. Schlegel, G. E. Scuseria, M. A. Robb, J. R. Cheeseman, G. Scalmani, V. Barone, G. A. Petersson, H. Nakatsuji, X. Li, M. Caricato, A. Marenich, J. Bloino, B. G. Janesko, R. Gomperts, B. Mennucci, H. P. Hratchian, J. V. Ortiz, A. F. Izmaylov, J. L. Sonnenberg, D. Williams-Young, F. Ding, F. Lipparini, F. Egidi, J. Goings, B. Peng, A. Petrone, T. Henderson, D. Ranasinghe, V. G. Zakrzewski, J. Gao, N. Rega, G. Zheng, W. Liang, M. Hada, M. Ehara, K. Toyota, R. Fukuda, J. Hasegawa, M. Ishida, T. Nakajima, Y. Honda, O. Kitao, H. Nakai, T. Vreven, K. Throssell, J. A. Montgomery, Jr., J. E. Peralta, F. Ogliaro, M. Bearpark, J. J. Heyd, E. Brothers, K. N. Kudin, V. N. Staroverov, T. Keith, R. Kobayashi, J. Normand, K. Raghavachari, A. Rendell, J. C. Burant, S. S. Iyengar, J. Tomasi, M. Cossi, J. M. Millam, M. Klene, C. Adamo, R. Cammi, J. W. Ochterski, R. L. Martin, K. Morokuma, O. Farkas, J. B. Foresman, D. J. Fox, Gaussian, Inc., Wallingford CT, **2016**.
[23] E. D. Glendening, J. K. Badenhoop, A. E. Reed, J. E. Carpenter, J. A. Bohmann, C. M. Morales, C. R. Landis, F. Weinhold, *Theoretical Chemistry Institute*, University of Wisconsin, Madison, **2013**.
[24] F. Weinhold, C. R. Landis, *Valency and Bonding A Natural Bond Orbital Donor-Acceptor Perspective*, Cambridge, University Press, Cambridge, **2005**.
[25] S. Grimme, J. Antony, S. Ehrlich, H. Krieg, *J. Chem. Phys.* **2010**, *132*, 154104.
[26] S. Ehrlich, J. Moellmann, W. Reckien, T. Bredow, S. Grimme, *ChemPhysChem* **2011**, *12*, 3414–3420.
[27] S. Grimme, A. Jansen, *Chem. Rev.* **2016**, *116*, 5105–5154.
[28] R. Ludwig, *Phys. Chem. Chem. Phys.* **2002**, *4*, 5481–5487.
[29] K. M. Murdoch, T. D. Ferris, J. C. Wright, T. C. Farrar , *J. Chem. Phys.* **2002**, *116*, 5717.
[30] R. Ludwig, *ChemPhysChem* **2005**, *6*, 1369–1375
[31] K. Fumino, S. Reimann, R. Ludwig, *Phys. Chem. Chem. Phys.*, **2014**, 40, 21903–21929.
[32] S. S. Xantheas, T. H. Dunning, *J. Chem. Phys.* **1993**, *99*, 8774–8792.
[33] A. B. Wolk, C. M. Leavitt, E. Garand, M. A. Johnson, *Acc. Chem. Res.* **2014**, *47*, 202–210.
[34] J. A. Fournier, C. T. Wolke, C. J. Johnson, A. B. McCoy, M. A. Johnson, *J. Chem. Phys.* **2015**, *142*, 064306.

Manuscript received: April 3, 2018
Accepted Article published: April 6, 2018
Version of record online: April 26, 2018